

# UC Davis

## UC Davis Previously Published Works

### Title

Ozone production in the upper troposphere and the influence of aircraft during SONEX: Approach of NO(x)-saturated conditions

### Permalink

<https://escholarship.org/uc/item/1br3n8br>

### Journal

Geophysical Research Letters, 26(20)

### ISSN

0094-8276

### Authors

Jaeglé, L  
Jacob, DJ  
Brune, WH  
[et al.](#)

### Publication Date

1999-10-15

### DOI

10.1029/1999GL900451

### Copyright Information

This work is made available under the terms of a Creative Commons Attribution License, available at <https://creativecommons.org/licenses/by/4.0/>

Peer reviewed

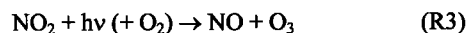
# Ozone production in the upper troposphere and the influence of aircraft during SONEX: Approach of NO<sub>x</sub>-saturated conditions

L. Jaeglé,<sup>1</sup> D.J. Jacob,<sup>1</sup> W.H. Brune,<sup>2</sup> I.C. Faloona,<sup>2</sup> D. Tan,<sup>2</sup> Y. Kondo,<sup>3</sup> G.W. Sachse,<sup>4</sup> B. Anderson,<sup>4</sup> G.L. Gregory,<sup>4</sup> S. Vay,<sup>4</sup> H.B. Singh,<sup>5</sup> D.R. Blake,<sup>6</sup> R. Shetter<sup>7</sup>

**Abstract.** During October/November 1997, simultaneous observations of NO, HO<sub>2</sub> and other species were obtained as part of the SONEX campaign in the upper troposphere. We use these observations, over the North Atlantic (40–60°N), to derive ozone production rates, P(O<sub>3</sub>), and to examine the relationship between P(O<sub>3</sub>) and the concentrations of NO<sub>x</sub> (= NO + NO<sub>2</sub>) and HO<sub>x</sub> (= OH + peroxy) radicals. A positive correlation is found between P(O<sub>3</sub>) and NO<sub>x</sub> over the entire data set, which reflects the association of elevated HO<sub>x</sub> with elevated NO<sub>x</sub> injected by deep convection and lightning. By filtering out this association we find that for NO<sub>x</sub> > 70 pptv, P(O<sub>3</sub>) is nearly independent of NO<sub>x</sub>, showing the approach of NO<sub>x</sub>-saturated conditions. Predicted doubling of aircraft emissions in the future will result in less than doubling of the aircraft contribution to ozone over the North Atlantic in the fall. Greater sensitivity to aircraft emissions would be expected in the summer.

## Introduction

In recent years, considerable attention has been given to the potential role of aircraft emissions of nitrogen oxides (NO<sub>x</sub> = NO + NO<sub>2</sub>) on the concentration of upper tropospheric ozone, an effective greenhouse gas [NASA, 1997]. Ozone is produced in the troposphere by the photochemical oxidation of CO and hydrocarbons which is catalyzed by NO<sub>x</sub> radicals and hydrogen oxide radicals (HO<sub>x</sub> = OH + peroxy). Oxidation of CO dominates in the upper troposphere, and the rate-limiting step for ozone production is the reaction of HO<sub>2</sub> with NO (R2):



The sensitivity of the ozone production rate, P(O<sub>3</sub>), to increasing NO<sub>x</sub> is critical to the assessment of aircraft effects. Photochemical models [e.g., Brasseur et al., 1996] predict that P(O<sub>3</sub>) should increase with increasing NO<sub>x</sub> (NO<sub>x</sub>-limited regime) up to a turnover point of a few hundred pptv NO<sub>x</sub>, beyond which further increases in NO<sub>x</sub> cause P(O<sub>3</sub>) to decrease (NO<sub>x</sub>-saturated regime). These two regimes result from the dual role of NO<sub>x</sub> in regulating the chemistry of HO<sub>x</sub> radicals. On the one hand, NO<sub>x</sub> drives the ozone production cycle (R1)–(R3). On the other hand, O<sub>x</sub> promotes the removal of HO<sub>x</sub> through reactions of OH with

HO<sub>2</sub>, HNO<sub>4</sub>, and NO<sub>2</sub> [Wennberg et al., 1998]. The chemical regime for ozone production is largely determined by the relative magnitudes of the sources of HO<sub>x</sub> and NO<sub>x</sub> [Jaeglé et al., 1998].

Ozone production rates in the upper troposphere have been previously determined from simultaneous measurements of HO<sub>2</sub> and NO during three recent aircraft campaigns: ASHORE/MAESA, STRAT and SUCCESS [Folkins et al., 1997; Wennberg et al., 1998; Brune et al., 1998; Jaeglé et al., 1998]. Examination of the P(O<sub>3</sub>) versus NO<sub>x</sub> relationships indicated a much greater prevalence for NO<sub>x</sub>-limited conditions than expected from models [Folkins et al., 1997; Jaeglé et al., 1998]. However, as we will see, interpretation of this relationship in terms of the chemical regime for ozone production can be biased by a commonality of sources for NO<sub>x</sub> and HO<sub>x</sub>.

We present here the first direct evidence of NO<sub>x</sub>-saturated conditions for ozone production in the upper troposphere and show that a simple interpretation of the observed P(O<sub>3</sub>) versus NO<sub>x</sub> relationship as a partial derivative  $\partial P(\text{O}_3)/\partial \text{NO}_x$  overestimates the actual sensitivity of ozone concentrations to emissions from aircraft. We use concurrent observations of HO<sub>2</sub> and NO obtained during the Subsonic assessment: Ozone and NO<sub>x</sub> Experiment (SONEX) DC-8 aircraft campaign. SONEX took place in October and November 1997 in the North Atlantic flight corridor, a region of dense aircraft traffic in the upper troposphere [Singh et al., this issue]. Companion papers use the SONEX data to improve our understanding of the chemistry and sources of NO<sub>x</sub> [Kondo et al., this issue; Thompson et al., this issue], and HO<sub>x</sub> [Brune et al., this issue].

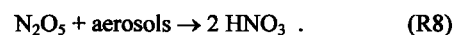
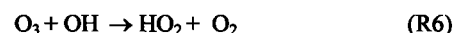
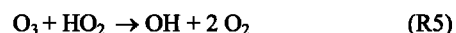
## Calculation of ozone production

Singh et al. [this issue] describe the flight tracks and the instruments aboard the DC-8 aircraft during SONEX. We focus here on observations made in the upper troposphere (8–12 km) between 40 and 60°N latitude, the main theater of operations. We exclude observations made in clouds (diagnosed by an abundance of particles larger than 3 μm), in fresh aircraft exhaust plumes (short duration peaks of elevated NO<sub>x</sub> and condensation nuclei), at high solar zenith angles (>80°), and in air masses with stratospheric influence (O<sub>3</sub> > 90 ppbv and CH<sub>4</sub> < 1760 ppbv).

We define the budget of ozone as that of the odd-oxygen family, O<sub>x</sub> (O<sub>x</sub> = O<sub>3</sub> + O + O(<sup>1</sup>D)) + NO<sub>2</sub> + HNO<sub>4</sub> + HNO<sub>3</sub> + 2NO<sub>3</sub> + 3N<sub>2</sub>O<sub>5</sub>), to account for rapid chemical cycling within this family. Ozone typically accounts for over 99% of O<sub>x</sub>, so the budgets of ozone and O<sub>x</sub> can be viewed as equivalent. In addition to reaction (R2), ozone can be produced by the reaction of organic peroxy radicals, RO<sub>2</sub>, with NO,



Ozone chemical loss is almost exclusively due to:



<sup>1</sup>Harvard University, Cambridge, Massachusetts.

<sup>2</sup>Pennsylvania State University, University Park.

<sup>3</sup>Nagoya University, Japan.

<sup>4</sup>NASA Langley Research Center, Hampton, Virginia.

<sup>5</sup>NASA Ames Research Center, Moffett Field, California.

<sup>6</sup>University of California, Irvine, California.

<sup>7</sup>National Center for Atmospheric Research, Boulder, Colorado.

The ozone production and loss rates,  $P(O_3)$  and  $L(O_3)$ , can thus be expressed as:

$$P(O_3) = k_2[HO_2][NO] + k_4[RO_2][NO] \quad (1)$$

$$L(O_3) = k_3[O_3][HO_2] + k_6[O_3][OH] + k_7[O(^1D)][H_2O] + k_8[N_2O_5], \quad (2)$$

where  $k_i$  is the rate constant for reaction ( $R_i$ ), and  $k_4$  is weighted over the different  $RO_2$  radicals contributing to ozone production. In the above expressions, we neglect the role of  $HNO_3+OH$ , which is a minor source of ozone (as per our definition of the  $O_x$  chemical family).

We use equations (1) and (2) with 1-minute averages of concurrent observations of  $NO$ ,  $HO_2$ ,  $OH$ ,  $H_2O$ ,  $O_3$ , UV actinic flux, aerosol surface area, temperature and pressure, to calculate instantaneous values of  $P(O_3)$  and  $L(O_3)$  along the flight tracks of the DC-8. For species which are not observed ( $RO_2$ ,  $O(^1D)$ ,  $N_2O_5$ ) we use calculations from a diel steady state model [Jaeglé *et al.*, 1998] constrained with local observations of  $O_3$ ,  $H_2O$ ,  $NO$ ,  $HNO_3$ , PAN, acetone,  $CO$ ,  $CH_4$ ,  $C_2H_6$ ,  $C_3H_8$ ,  $C_4$  alkanes, UV actinic flux, aerosol surface area, temperature and pressure. The resulting instantaneous  $P(O_3)$  and  $L(O_3)$  rates are then scaled to 24-hour average values by using local results from the diel steady state model:

$$\langle Rate_{obs} \rangle_{24h} = Rate_{obs}(t) \times \langle Rate_{model} \rangle_{24h} / Rate_{model}(t), \quad (3)$$

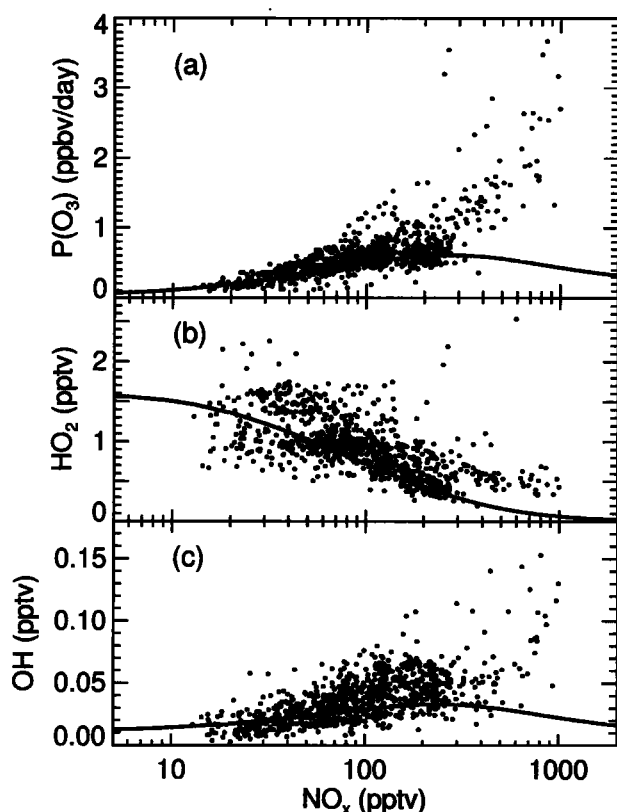


**Figure 1.** Observed ozone production rates  $P(O_3)$ , and concentrations of  $HO_2$  and  $OH$  in SONEX (8–12 km altitude, 40–60°N latitude) plotted as a function of the  $NO_x$  concentration ( $NO_x = \text{observed } NO + \text{modeled } NO_2$ ). The observed rates and concentrations are averaged over 24 hours, using diel factors obtained from a locally constrained photochemical model. The lines on the three panels correspond to model-calculated values for median upper tropospheric background conditions during SONEX (see text).

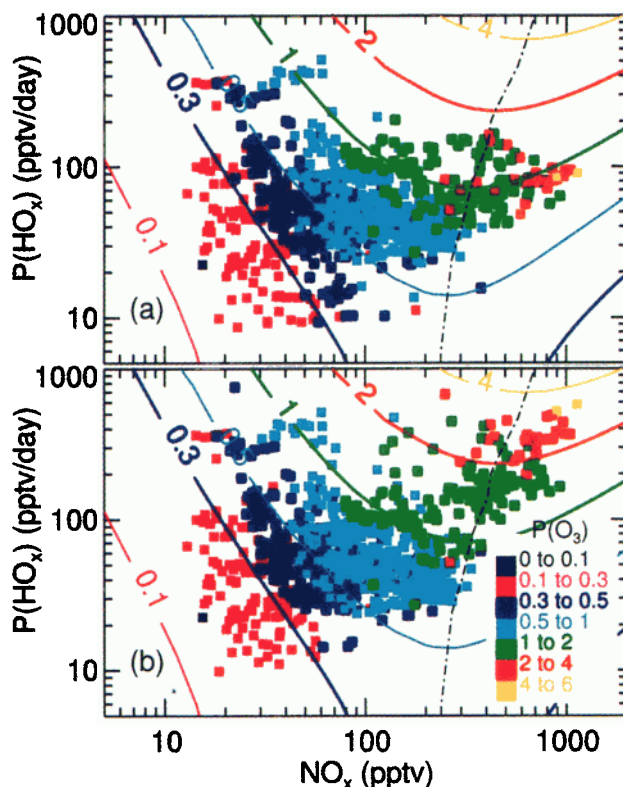


**Figure 2.** Ozone production rate  $P(O_3)$  (ppbv/day) in SONEX as a function of  $NO_x$  mixing ratio and the primary  $HO_x$  source,  $P(HO_x)$ , in the upper troposphere (8–12 km). The contour lines correspond to model calculations of 24-hour average  $P(O_3)$  for background conditions during SONEX. Values of  $P(O_3)$  computed from observed  $NO$  and  $HO_2$  and scaled to 24-hour averages (see Figure 1) are shown as color-coded squares. In panel a, the values of  $P(HO_x)$  corresponding to the observed  $P(O_3)$  are calculated using the observed concentrations of  $H_2O$  and acetone. In panel b,  $P(HO_x)$  was increased in order to match the observations of  $HO_2$  where required (see text). The dashed line corresponds to  $\partial P(O_3)/\partial NO_x = 0$ .

A more detailed description of the model as applied to SONEX observations can be found in Jaeglé *et al.* [Photochemistry of  $HO_x$  in the upper troposphere at northern midlatitudes, submitted to *J. Geophys. Res.*, 1999, hereafter referred to as J99].

### Relationships between $NO_x$ , $HO_x$ , and ozone production

Figure 1a shows the relationship between the 24-hour average values of  $P(O_3)$  derived from observed  $HO_2$  and  $NO$ , and the local  $NO_x$  concentrations in the upper troposphere (8–12 km) between 40°N and 60°N latitude. The calculated median  $P(O_3)$  for SONEX was 0.57 ppbv/day. The median  $L(O_3)$  was 0.13 ppbv/day (not shown here), resulting in a net ozone production of 0.44 ppbv/day. Reaction of  $NO$  with  $HO_2$  dominates ozone production; reaction ( $R_4$ ) contributes on average less than 15% of the total  $P(O_3)$ . Reactions of  $O_3$  with  $HO_2$  and  $OH$  contribute more than 80% of  $L(O_3)$ , while reactions ( $R_7$ ) and ( $R_8$ ) contribute 10% and 5% respectively.

The line in Figure 1a shows the expected dependence of ozone production on  $NO_x$  for diel steady state model calculations where

model input variables are specified from median background conditions observed during SONEX at 10 km [J99]: 55 ppbv  $O_3$ , 120 ppmv  $H_2O$ , 120 pptv  $HNO_3$ , 64 pptv PAN, 510 pptv acetone, 90 ppbv CO, 1761 ppbv  $CH_4$ , 670 pptv  $C_2H_6$ , 79 pptv  $C_3H_8$ , 55 pptv  $C_4$  alkanes, 50°N latitude, 285 DU ozone column,  $8 \mu m^2 cm^{-3}$  aerosol surface area, 227 K temperature, on November 1. In the model,  $P(O_3)$  becomes relatively independent of  $NO_x$  above 70 pptv; and the turnover to the  $NO_x$ -saturated regime ( $\partial P(O_3)/\partial NO_x = 0$ ) takes place at 300 pptv. The bulk of the observations ( $NO_x < 300$  pptv) shows indeed a leveling off of the dependence of  $P(O_3)$  on  $NO_x$  as  $NO_x$  increases above 70 pptv, in accordance with the expected behavior. However, for the highest  $NO_x$  concentrations, the values of  $P(O_3)$  computed from observed  $HO_2$  and NO continue to increase with increasing  $NO_x$ , suggesting a consistently  $NO_x$ -limited regime which is at odds with model results.

The largest  $NO_x$  concentrations (>300 pptv) shown in Figure 1 correspond to relatively fresh convective outflows sampled close to the U.S. East coast [Thompson *et al.*, this issue]. Elevated  $NO_x/NO_y$  ratios (>0.5 mol/mol), backtrajectory calculations and satellite lightning imagery all support a strong source of  $NO_x$  from lightning associated with this convection [Pickering *et al.*, 1999]. These air masses were also characterized by an enhanced  $HO_x$  source resulting from convective transport of surface air with elevated concentrations of  $HO_x$  precursors such as peroxides and  $CH_2O$  [J99]. Based on (1), comparison between observed and modeled  $P(O_3)$  for a given  $NO_x$  concentration is roughly equivalent to comparison of observed and modeled  $HO_2$  concentrations. We see from Figure 1b that the model constrained with background conditions for SONEX underestimates  $HO_2$  by a factor of two or more when  $NO_x > 300$  pptv. Using the locally observed concentrations of  $HO_x$  precursors ( $H_2O$ , acetone, peroxides and  $CH_2O$ ) for these high- $NO_x$  points improves the agreement but still comes short of the observed levels. The discrepancy suggests the presence of other unmeasured sources, such as higher aldehydes, possibly also resulting from convection [Müller and Brasseur, 1999]. It could also reflect flaws in our understanding of  $HO_x$  chemistry in the high- $NO_x$  regime [Faloona *et al.*, 1999], or other unknown  $HO_x$  sources [Chatfield *et al.*, 1999]. For the remaining observations ( $NO_x < 300$  pptv), the dependence of  $HO_2$  and OH on  $NO_x$  is generally well reproduced (Fig. 1b and 1c). The scatter around the model lines in Figure 1 can be explained by variations in the magnitude of the local  $HO_x$  sources [J99].

In models of the upper troposphere,  $P(O_3)$  is largely determined by two variables:  $NO_x$  mixing ratios and the strength of the primary  $HO_x$  source,  $P(HO_x)$  [Jaeglé *et al.*, 1998]. Figure 2 shows the variations of  $P(O_3)$  as a function of  $NO_x$  and  $P(HO_x)$ . We separate primary sources (i.e. sources independent of  $HO_x$ ) from secondary sources (i.e. sources dependent on a preexisting pool of  $HO_x$ ), and define the primary  $HO_x$  source as:

$$P(HO_x) = 2k_7[O(^1D)][H_2O] + y_{acet}J_{acet}[Acetone] + \sum y_{X_i}J_{X_i}[X_i], \quad (4)$$

where  $J_{acet}$  and  $y_{acet}$  are the photolysis rate constant and  $HO_x$  yield for acetone, and  $J_{X_i}$  and  $y_{X_i}$  are the photolysis rate constants and  $HO_x$  yields for other convected  $HO_x$  precursors such as peroxides and aldehydes (see Müller and Brasseur [1999] for this definition of the primary  $HO_x$  source). The value of  $y_{acet}$  is about three [Singh *et al.*, 1995]. Methane oxidation by OH, and the subsequent photolysis of  $CH_2O$  was an important  $HO_x$  source during SONEX [J99]. We do not include this source in our definition of  $P(HO_x)$  because it is a secondary  $HO_x$  source.

In Figure 2a, we calculate  $P(HO_x)$  based on the observed  $H_2O$  and acetone.  $P(HO_x)$  is averaged over 24 hours using (3). In Figure 2b, in addition to  $H_2O$  and acetone, we include an additional  $HO_x$  source ( $\sum y_{X_i}J_{X_i}[X_i]$ ) as required to match the observed  $HO_2$  concentrations. This source might include contributions from convected peroxides and aldehydes, which we

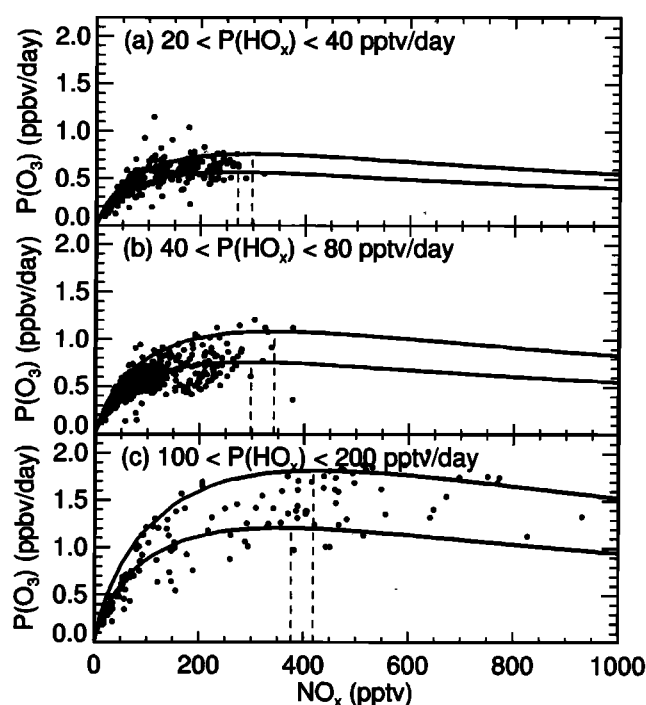


**Figure 3.** Observed ozone production rate in SONEX (24-hour average) as a function of  $NO_x$  mixing ratios for three ranges of the primary  $HO_x$  production  $P(HO_x)$ : (a) 20–40 pptv/day, (b) 40–80 pptv/day, (c) 100–200 pptv/day. Model calculations corresponding to the limits of each range are also shown. Note the linear scale for  $NO_x$ . The dashed lines correspond to  $\partial P(O_3)/\partial NO_x = 0$ .

cannot easily quantify from our model. Its impact on  $P(HO_x)$  is small (less than 50%) except for observations in continental convective outflows with elevated  $NO_x$  (15% of the points in Figure 2b). As seen in Figure 2, model calculations of  $P(O_3)$  for median background SONEX conditions with varying  $NO_x$  and  $P(HO_x)$  (contour lines) generally reproduce the observations (square symbols).

The primary  $HO_x$  source in the SONEX data displays large variations, with 24-hour average values ranging from 10 pptv/day to 700 pptv/day (Fig. 2). Elevated  $P(HO_x)$  values (200–700 pptv/day) are sometimes associated with low  $NO_x$  concentrations (<30–40 pptv). These air masses were influenced by recent marine convection and high concentrations of water vapor; despite the enhanced source of  $HO_x$ , the low levels of  $NO_x$  result in relatively low  $P(O_3)$  (0.1–0.5 ppbv/day). Elevated  $P(HO_x)$  is also found in association with high  $NO_x$  concentrations (>300 pptv). As noted above, the elevated  $NO_x$  was the result of recent lightning and convection, and concurrent enhancement of  $P(HO_x)$  would be expected from the convective injection of  $HO_x$  precursors. The positive correlation between high  $NO_x$  and  $P(HO_x)$  in the observations is particularly apparent in Figure 2b, but can also be seen in Figure 2a. This correlation results in the highest levels of  $P(O_3)$  observed. By supplying  $HO_x$  precursors together with  $NO_x$ , deep convection extends the  $NO_x$ -limited regime to higher concentrations of  $NO_x$ .

### Chemical regime for ozone production

To diagnose the actual dependence of  $P(O_3)$  on  $NO_x$  in the SONEX observations, the additional sensitivity to  $P(HO_x)$  must be resolved. We therefore examined the dependence of  $P(O_3)$  on  $NO_x$  for similar primary  $HO_x$  production rates. Figure 3 illustrates this dependence for three ranges of  $P(HO_x)$ . The  $P(HO_x)$  values used to segregate the observations are those required in order to match the observed  $HO_2$  (Fig. 2b). Choosing

instead the  $P(\text{HO}_x)$  values computed from  $\text{H}_2\text{O}$  and acetone only (Fig. 2a) results in some small differences in Figure 3c.

Figure 3 shows that  $P(\text{O}_3)$  derived from observations increases nearly linearly with  $\text{NO}_x$  for  $\text{NO}_x < 70$  pptv. In Figures 3a and 3b,  $P(\text{O}_3)$  shows very little dependence on  $\text{NO}_x$  between 70 pptv and 300 pptv, approaching the  $\text{NO}_x$ -saturated regime. The bin with the highest levels of  $P(\text{HO}_x)$  (Fig. 3c), shows a positive dependence of  $P(\text{O}_3)$  on  $\text{NO}_x$  extending to a higher  $\text{NO}_x$  concentration (200 pptv) but there is still clear evidence of  $\text{NO}_x$ -saturated conditions beyond this. The median  $\text{NO}_x$  mixing ratio was 93 pptv in the upper troposphere (8–12 km) during SONEX, and the median  $P(\text{HO}_x)$  was 50 pptv/day. These conditions correspond to a regime where ozone production is less sensitive to changes in  $\text{NO}_x$ .

Because of the slow photochemistry in October–November and the elevated levels of  $\text{NO}_x$ , the conditions during SONEX allowed extensive sampling of the transition region between the  $\text{NO}_x$ -limited and  $\text{NO}_x$ -saturated regimes as illustrated in Figure 3. Previous aircraft campaigns (ASHOE/MAESA, STRAT, SUCCESS), where ozone production was consistently  $\text{NO}_x$ -limited, featured lower  $\text{NO}_x$  concentrations and more active photochemistry. In the tropical upper troposphere during STRAT,  $\text{NO}_x$  mixing ratios were generally less than 100 pptv [Wennberg et al., 1998]. Over the central United States during SUCCESS, springtime conditions resulted in more rapid photochemistry compared to SONEX and thus a higher transition from  $\text{NO}_x$ -limited to  $\text{NO}_x$ -saturated regimes ( $\text{NO}_x \sim 500$  pptv) [Jaeglé et al., 1998].

Delineation of the regimes for ozone production is critical when assessing the effect of aircraft emissions. Aircraft, unlike deep convection and lightning, inject  $\text{NO}_x$  into the upper troposphere without injecting  $\text{HO}_x$  precursors (the aircraft sources of  $\text{H}_2\text{O}$  and  $\text{HONO}$  are negligibly small [NASA, 1997]). As summarized in Singh et al. [this issue], aircraft emissions might have contributed 20–70% of the observed  $\text{NO}_x$  in the upper troposphere during SONEX. A 40% aircraft effect corresponds to a 37 pptv contribution to the median observed  $\text{NO}_x$  concentration of 93 pptv. Based on the dependence shown in Figure 3b, and assuming a SONEX median value for  $P(\text{HO}_x)$  of 50 pptv/day, such a  $\text{NO}_x$  increase results in an increase of  $P(\text{O}_3)$  from 0.45 to 0.6 ppbv/day. For a 2-week residence time of air in the upper troposphere at midlatitudes, this increase of 0.15 ppbv/day adds about 2.1 ppbv of ozone, resulting in a 4% increase in upper tropospheric ozone in the north Atlantic flight corridor in the fall. For a larger range of  $P(\text{HO}_x)$  values (20–100 pptv/day), the increase in ozone is 2–6%.

A further doubling of  $\text{NO}_x$  concentrations due to future aircraft emissions ( $\text{NO}_x = 93 + 37$  pptv) would only result in an additional 0.1 ppbv/day ozone production under SONEX conditions (northern midlatitudes in the fall) because of the  $\text{NO}_x$ -saturated regime. However, if the primary source of  $\text{HO}_x$  were to rise in the future,  $P(\text{O}_3)$  would become more sensitive to increases in  $\text{NO}_x$  from aircraft emissions. As noted above, during summer the transition to  $\text{NO}_x$ -saturated regime occurs at higher levels of  $\text{NO}_x$ , and thus increases in aircraft emissions should continue to result in  $\text{O}_3$  increases in the foreseeable future [NASA, 1997].

## Conclusions

We computed ozone production rates  $P(\text{O}_3)$  in the upper troposphere at northern midlatitudes, using simultaneous observations of  $\text{HO}_2$  and  $\text{NO}$  during SONEX (October–November 1997). High levels of  $\text{NO}_x$  due to lightning and convection were associated with high concentrations of  $\text{HO}_x$  precursors also supplied by convection. The observed correlation between elevated  $\text{NO}_x$  and  $\text{HO}_x$  sources resulted in a positive relationship between  $P(\text{O}_3)$  and  $\text{NO}_x$  extending over the full range of  $\text{NO}_x$  concentrations observed (up to 1 ppbv). By segregating the data

according to the primary  $\text{HO}_x$  production rate,  $P(\text{HO}_x)$ , we find that ozone production in fact approached  $\text{NO}_x$ -saturated conditions for  $\text{NO}_x$  concentrations larger than 70 pptv. This result implies little sensitivity of  $P(\text{O}_3)$  to future increases in  $\text{NO}_x$  emissions from aircraft (which unlike convective injection are not associated with a large source of  $\text{HO}_x$ ) during the fall at northern midlatitudes. A greater sensitivity of  $P(\text{O}_3)$  to  $\text{NO}_x$  would be expected under summer conditions.

**Acknowledgments.** This work was supported by the Subsonic Assessment Program (SASS) of the National Aeronautics and Space Administration (NASA).

## References

- Brasseur, G., J.-F. Müller, and C. Granier, Atmospheric impact of  $\text{NO}_x$  emissions by subsonic aircraft: a three-dimensional model study, *J. Geophys. Res.*, **101**, 1423–1428, 1996.
- Brune, W.H., et al., Airborne in-situ OH and  $\text{HO}_2$  observations in the cloud-free troposphere and lower stratosphere during SUCCESS, *Geophys. Res. Lett.*, **25**, 1701–1704, 1998.
- Brune, W.H., et al., OH and  $\text{HO}_2$  chemistry in the North Atlantic free troposphere, *Geophys. Res. Lett.*, this issue, 1999.
- Chatfield, R.B., et al., Attributing sources for  $\text{NO}_x$  observed in the Atlantic free troposphere during the SONEX period: models and observations emphasize effects of aircraft, *submitted to J. Geophys. Res.*, 1999.
- Faloona, I., et al., Observation of  $\text{HO}_x$  and its relationship with  $\text{NO}_x$  in the upper troposphere during SONEX, *submitted to J. Geophys. Res.*, 1999.
- Folkens, I., et al., OH and  $\text{HO}_2$  in two biomass burning plumes: source of  $\text{HO}_x$  and implications for ozone production, *Geophys. Res. Lett.*, **24**, 3185–3188, 1997.
- Jaeglé, L., et al., Sources of  $\text{HO}_x$  and production of ozone in the upper troposphere over the United States, *Geophys. Res. Lett.*, **25**, 1705–1708, 1998.
- Kondo, Y., et al., Impact of aircraft emissions on  $\text{NO}_x$  in the lowermost stratosphere at northern midlatitudes, *Geophys. Res. Lett.*, this issue, 1999.
- Müller, J.-F., and G. Brasseur, Sources of upper tropospheric  $\text{HO}_x$ : A three-dimensional study, *J. Geophys. Res.*, **104**, 1705–1715, 1999.
- Pickering, K.E., et al., Comparison and interpretation of chemical measurements from two SONEX flights over the Canadian maritime: Lightning, convection and aircraft signatures, *submitted to J. Geophys. Res.*, 1999.
- National Aeronautics and Space Administration, Atmospheric effects of aviation, *Interim assessment report of the advanced subsonic technology program*, Ref. Publ. 1400, 1997.
- Singh, H.B., et al., High concentrations and photochemical fate of oxygenated hydrocarbons in the global troposphere, *Nature*, **378**, 50–54, 1995.
- Singh, H.B., A.M. Thompson, and H. Schlager, SONEX airborne mission and coordinated POLINAT-2 activity: Overview and accomplishments, *Geophys. Res. Lett.*, this issue, 1999.
- Thompson, A.M., et al., Fingerprinting  $\text{NO}_x$  in SONEX: What was the aircraft contribution to  $\text{NO}$  sources? *Geophys. Res. Lett.*, this issue, 1999.
- Wennberg, P.O., et al., Hydrogen radicals, nitrogen radicals and the production of ozone in the middle and upper troposphere, *Science*, **279**, 49–53, 1998.
- D. Blake, Department of Chemistry, University of California, Irvine, CA 92717.
- W. Brune, I. Faloona, D. Tan, Pennsylvania State University, Department of Meteorology, University Park, PA 16802.
- D. Jacob, L. Jaeglé (corresponding author), Division of Engineering and Applied Sciences, and Department of Earth and Planetary Sciences, Harvard University, 29 Oxford Street, Pierce Hall, Cambridge, MA 02138. (e-mail: lyj@io.harvard.edu)
- Y. Kondo, Solar Terrestrial Environment Laboratory, Nagoya University, Japan.
- G. Sachse, B. Anderson, G. Gregory, S. Vay, NASA Langley Research Center, Hampton, VA 23665.
- R. Shetter, National Center for Atmospheric Research, Boulder, CO 80307.
- H. Singh, NASA Ames Research Center, Moffett Field, CA 94035.

(Received March 8, 1999; revised May 13, 1999; accepted May 14, 1999)